TÜBİTAK

Turk J Phys
35 (2011) , 129 – 135.

doi:10.3906/fiz-1010-13

Study of differential cross section using different bound state potentials

Ass'ad I. ASS'AD
Department of physics, Faculty of Applied science, Al-Aqsa University,
Gaza Strip-PALESTINIAN AUTHORITY
e-mail: assad_assad11@yahoo.com

Received: 04.11.2010

Abstract

In this study, heavy ion reactions of ^{6}Li + (^{58}Ni, ^{28}Si ,^{12}C) and ^{7}Li + ^{12}C are studied using different bound state potentials, within the framework of the Distorted Wave Bourn Approximation (DWBA) calculations. Woods-Saxon potential is expressed as the optical potential in the initial and final channels together with a Coulomb potential. The calculations of the angular distributions are found to be in a good agreement with the experimental data. The extracted spectroscopic factors are reasonable.

Key Words: Different bound state potentials, angular distributions, Woods-Saxon potential

1. Introduction

Heavy ion scattering and the scattering of nucleons from nuclei have been widely considered in the last few years [1]. Elastic scattering is a basic process in nuclear collisions because it accompanies another reaction mechanism, and a thorough understanding of elastic scattering is a prerequisite for a valid description of nonelastic processes [2]. At energies near the Coulomb barrier usually it have been shown an anomalous behavior of the energy dependence of the real and imaginary parts of the optical potential, known as the threshold anomaly [3]. This anomaly shows up as a localized peak in the real part and the decreasing and vanishing of the imaginary part of the potential in the neighborhood of the Coulomb barrier [4, 5]. The decrease of the imaginary potential as one approaches the Coulomb barrier is due to the closing of the effective open channels which can lead to absorption of flux from the elastic channel. Recently, extensive theoretical calculations have been done to explain the resonant structures, which usually observed in heavy ion transfer reaction, following the microscopic distorted wave Born approximation (DWBA) calculation [6, 7], where DWBA was used to widely study in direct nuclear reactions [8]. For most cases the DWBA is one step process [9]. Therefore, several descriptions have been introduced to explain the general features of heavy-ion reactions [10]. The investigation of nuclear structure effects in the fusion cross section has deserved special attention in the last few years. In the case of the study of sub-barrier fusion reactions, the standard models based on the penetrability of one dimensional barriers determined by the ion-ion potential were systematically used [11].

^{12}C + ^{92}Zr and ^{16}O + ^{92}Zr systems have been studied using the fusion coupled-channel calculations. At energies near the Coulomb barrier, calculations have been quite successful [12]. The elastic scattering for ^{46,50}Ti(^{16}O, ^{16}O) systems investigated in the sub-Coulomb fusion of heavy-ions demand a careful investigation of the reaction cross section and optical potentials near the Coulomb barrier [11]. Differential cross-sections of reactions ^{24}Mg(^{16}O,^{16}O)^{24}Mg and ^{28}Si(^{16}O,^{16}O)^{28}Si can be found agreement with experimental data for the whole angle region in both cases.

In the elastic scattering between $4N$ nuclei, such as the ^{24}Mg(^{16}O,^{16}O)^{24}Mg case, an uprising oscillatory structure often appears in the differential cross-section at the backward angle region [13].

The (^{7}Li, ^{6}He) reactions are considered a valuable spectroscopic tool because the shapes of their angular distributions can be well reproduced by the distorted wave Born approximation (DWBA) [14]. The angular distributions for low lying states of ^{16}O produced in the ^{12}C(^{6}Li, d)^{16}O α-transfer reaction at incident energy 48.28 MeV have been measured using a high energy resolution position sensitive detection system [15].

The present work considers the theory of heavy–ion induced reactions with particle transfer. These direct transfer reactions are investigated using the exact finite-range DWBA calculations as a single-step process. The optical model potential is taken to have real and imaginary Woods-Saxon form in the initial and final channels plus the Coulomb potential. The calculated differential cross sections are fitted with the experimental data to extract spectroscopic factors

2. Differential cross sections

In the present calculations, the explicit transition matrix element of the $T(A,C)R$ reaction with a transferred particle x are evaluated in details following the DWBA calculations [16,17]. Therefore, the complete reaction transition is taken to have the expression

$$T_{fi} = \sum_{lj,l'j'} S(l,j)\, S^{*}(l',j') \cdot \langle J_C \mu_C\,;\, J_R \mu_R\ (J'_x j'\,(J,l'))|\, T^{ll'}\ |(J_C\,\mu\, J_A\,\mu_A\,;\, J_T\,\mu_T\,(J_X\, j(J_C\, l))\rangle\,, \qquad (1)$$

where $S(l,j)$ and $S^{*}(l',j')$ are the spectroscopic factors in the initial and final channels respectively; J_i and μ_i are the respective spin angular momenta of particle i and its magnetic projection on the z-component. In these calculations, the standard Woods-Saxon forms [18] are used for the real and imaginary distorting potential in the initial and final channels together with a Coulomb potential. The nucleus-nucleus potential is given as

$$V(r) = -\ V\, f(r, r_v, a_v) - iW f\,(r, r_w, a_w)\ +\ V^{C}(r) \qquad (2)$$

where $f(r, r_x, a_x)$ is the Woods- Saxon form factor and is expressed as

$$f(r, r_x, a_x) = \left[1 + \exp\left(\frac{r - R_x}{a_x}\right)\right]^{-1} \qquad \text{for}\ \ x = v, w, c. \qquad (3)$$

Coulomb potential $V^{C}(r)$ is due to a uniform sphere of radius r_C= 1.25 fm and is given as

$$V^{C}(r) = \begin{cases} Z_i Z_j\, e^2\left(3 - r^2/R_C^2\right)/2R_C & ;\quad r \le R_C \\ Z_i Z_j e^2/r & ;\quad r \ge R_C. \end{cases} \qquad (4)$$

In such calculations, the imaginary part of the optical potential is taken to have the form

$$W(r) = \left[i \left(w \; - \; 4 w_D a_w \, \frac{d}{dr_w} \right) \right] \, f\left(r, r_w, a_w\right). \tag{5}$$

In terms of the complete transition amplitude, the differential cross section for heavy ion reactions with particle transfer is given as

$$\frac{d\sigma}{d\Omega} \;=\; \frac{M_{AT} M_{XR}}{\left(2\pi\hbar^2\right)^2} \; \frac{k_f}{k_i} \frac{1}{\left(2\,J_A + 1\right)\left(2 J_R + 1\right)} \sum_{\substack{\mu_A, \mu_T \\ \mu_R, \mu_C}} |T_{fi}|^2, \tag{6}$$

where M_{ij} is the reduced mass of particles i and j; the μ's are the magnetic quantum numbers; and K_i and K_j are the relative momenta in the initial and final channels respectively.

3. Numerical calculations and results

In the present calculations, the ^{6}Li projectile is assumed as a bound state of ^{58}Ni, ^{28}Si, ^{12}C at incident energy 210 MeV and the ^{7}Li projectile is assumed as a bound state of ^{12}C at incident energy 132 MeV. In the first set of the present calculations the particle-particle interactions of the bound states in the initial and final channels are described in terms of double-Gaussian potentials; in the second set, it is described by the Yukawa potential [19].

The Gaussian potentials has the form

$$V(r) = V_{Ri} \exp\left(-r_i^2/a_{Ri}^2\right) \; + \; V_{Ai} \exp\left(-r_i^2/a_{Ai}^2\right) \; ; \quad i = 1,\, 2, \tag{7}$$

where, $V_{Ri} > 0$ and $V_{Ai} < 0$ are the strengths of the repulsive and attractive terms respectively, while a_{Ri} and a_{Ai} are their decay factors. These parameters are listed in Table 1. While the Yukawa potential has the form

$$V_{ij}(r_{ij}) = V_{ij}^0 \left(2 + \; \frac{r_{ij} \; - (R_i \; + \; R_j)}{a} \right) e^{\frac{-r_{ij} \, + R_i \, + \, R_j}{a}}, \tag{8}$$

where R_i and R_j are the radii of the i^{th} and j^{th} particles given by $r_o A^{1/3}$, V_{ij}^0 represents the interaction strength given as

$$V_{ij}^0 = \left[C(i)\, C(j)\right]^{\frac{1}{2}} \; \frac{a\, R_i\, R_j}{r_0^2\, (R_i + R_j)}. \tag{9}$$

The parameter $C(i)$ in equation (9) has the value

$$C(i) = A(i) \left[1 - K_s \left(\frac{N_i - Z_i}{A_i} \right)^2 \right], \tag{10}$$

with a similar expression introduced for the parameter $C(j)$.

The different parameters of the interactions are given as $r_0 = 1.18$ fm, $a = 0.65$ fm, $A(i) = 21.17$ MeV, and the surface a symmetry constant $K_s = 3.0$, which are chosen to fit the static properties of nuclei [19]. The necessary parameters of the optical potential are listed in Tables 2 and 3.

Table 1. Parameters of the double Gaussian potential.

Reaction	V_R	a_R	V_A	a_A	a_{Ho}
	(MeV)	(fm)	(MeV)	(fm)	(fm)
^{6}Li + ^{58}Ni	209	1.30	-210	1.80	1.55
^{6}Li + ^{28}Si	209	1.20	-200	1.90	1.50
^{6}Li + ^{12}C	219	1.80	-210	1.40	1.50
^{7}Li + ^{12}C	209	1.70	-210	1.30	1.50

Table 2. Optical potential parameters used in the DWBA calculations.

Reaction	V_0	R_v	a_v	W_0	R_w	a_w	r_c
	(MeV)	(fm)	(fm)	(MeV)	(fm)	(fm)	(fm)
^{6}Li +^{58}Ni	174.5	1.136	0.907	32.0	1.607	0.806	1.5
^{6}Li +^{28}Si	176.5	1.3	0.7	32.9	1.7	0.9	1.4
^{6}Li +^{12}C	113.5	1.305	0.793	34.2	1.682	0.784	1.5
^{7}Li +^{12}C	132	1.6	0.960	31.5	1.607	0.806	1.25

Table 3. Extracted spectroscopic factors.

Reaction	Incident energy (MeV)	Excitation energy (MeV)	J^π	Spectroscopic factors	
				Present	Previous
^{6}Li +^{58}Ni	27.80	0.0	0^+	0.91	0.79
^{6}Li + ^{28}Si	36.26	0.0	0^+	0.94	0.78
^{6}Li + ^{12}C	27.75	0.0	0^+	0.78	0.74
^{7}Li + ^{12}C	26.23	0.0	0^+	0.82	0.79

The result obtained for the differential cross sections are shown in Figures 1–4 by solid curves (Gaussian potential) and dashed lines (Yukawa potential) compared with the experimental data points. Generally, the present calculations using Gaussian potential provide a substantially better description of the phase and magnitude of the angular distributions than the Yukawa potential.

In comparison, using both Gaussian and Yukawa potentials, the angular distribution are found to be in a good agreement with the experimental data in the forward region as shown in the figures. In addition, calculations employing Gaussian potentials give an equivalent fit to the experimental data in the large angle region as shown in Figures 1, 2, and 4 and also introduce a description better than those using Yukawa potentials. Generally, these calculations grossly overestimate the cross-sections at the back-angle region as shown in Figure 3. By matching the present theoretical calculations of the differential cross-sections with the experimental data, the spectroscopic factors in each reaction state are extracted as

$$S(l,j) = \frac{1}{N_S}\,\frac{(2J_i+1)}{(2\,J+1)}\,\frac{\left(\frac{d\sigma}{d\Omega}\right)_{\rm exp.}}{\left(\frac{d\sigma}{d\Omega}\right)_{\rm theor.}}. \tag{11}$$

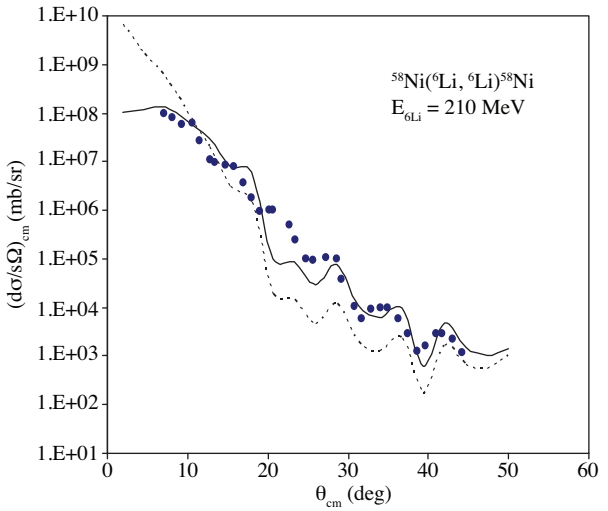

Figure 1. Differential cross-section of the ^{58}Ni (^{6}Li, ^{6}Li) ^{58}Ni reaction at 210 MeV incident energy leading to 0.0 ^{58}Ni excited state. The solid curve denotes the Gaussian potential. The dotted line denotes the Yukawa potential and the dots are the experimental data taken from reference [20].

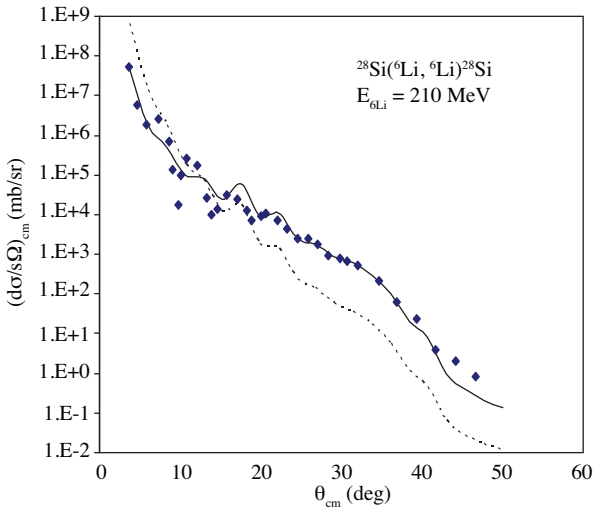

Figure 2. The differential cross-section of the ^{28}Si (^{6}Li, ^{6}Li) ^{28}Si reaction at 210 MeV incident energy leading to 0.0 ^{28}Si excited state. The solid curve denotes the Gaussian potential. The dotted line denotes the Yukawa potential and the dots are the experimental data taken from reference [20].

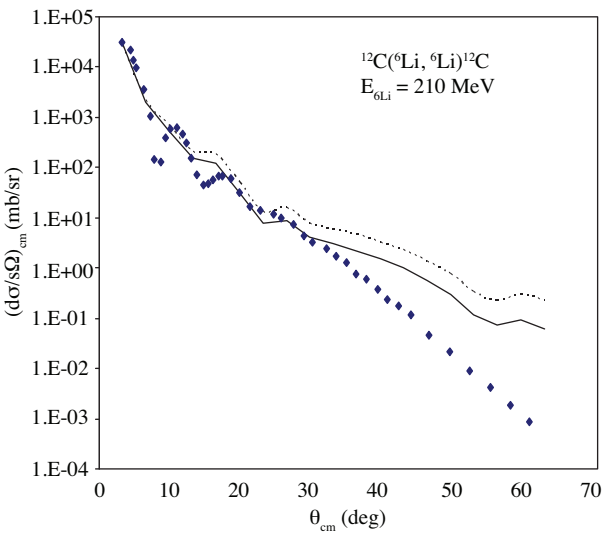

Figure 3. The differential cross-section of the ^{12}C (^{6}Li, ^{6}Li) ^{12}C reaction at 210 MeV incident energy leading to 0.0 ^{12}C excited state. The solid curve denotes the Gaussian potential. The dotted line denotes the Yukawa potential and the dots are the experimental data taken from reference [21].

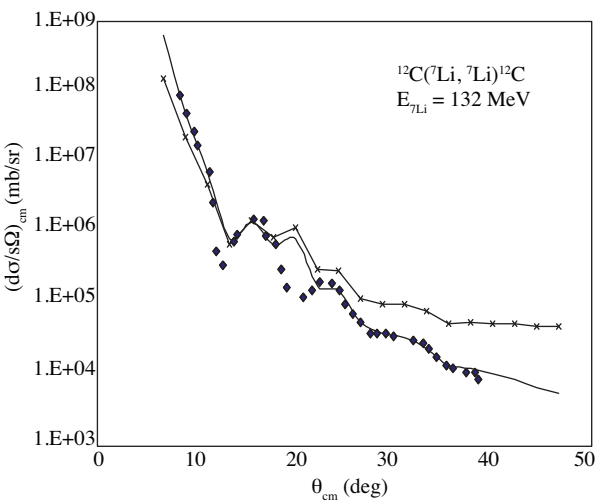

Figure 4. The differential cross-section of the ^{12}C (^{7}Li, ^{7}Li) ^{12}C reaction at 132 MeV incident energy leading to 0.0 ^{12}C excited state. The solid curve denotes the Gaussian potential. The dotted line denotes the Yukawa potential and the dots are the experimental data taken from reference [20].

4. Discussion and conclusion

In the present work, different heavy-ion transfer reactions have been studied within the framework of the DWBA calculations using optical potential model. The calculated angular distributions using both of Gaussian potentials and Yukawa potentials are found to be in a good agreement with the experimental data in the forward angle region. In general, although the calculated forward cross-sections are found to be equivalent and close enough in such cases, the using of the Gaussian potentials introduces a substantially better description of the large angle data than using of Yukawa potentials. Therefore, the present analysis exhibits the Gaussian potentials term to account for the phase and amplitude of the angular distributions as well as the magnitude of the cross-sections at large angular range.

We conclude that the present one-step DWBA process, using the Woods-Saxon form as optical potential, and the double Gaussian potential as bound states, exhibit reasonably good fits to the experimental data and satisfactory reproduce both of the magnitude and shapes of the differential cross-sections in the forward and large angle regions.

References

[1] A. Osman, *Acta Physica Polonica B,* **40**, (2009), 2345.

[2] B. Zhen, *Chin.Phys.Lett.*, **24**, (2007), 3384.

[3] Y. Sugiyama, *Japanese Nuclear Data Committee and Nuclear Data Center*, **March 1992**, (1993), 82.

[4] P. Gomes, R. Anjos, R. Muri, C. Lubian and I. Padron, *Phys. Rev. C* , **70**, (2004), 1.

[5] L. Chamon, M. Hussein and L. Canto, *Braz. J. Phys.*, **37**, (2007), 1177.

[6] A. Farra, *Turk. J. Phys.*, **27**, (2003), 241**.**

[7] I. Ass'ad and H. Ashour, *J. of Applied Sciences*, **7**, (2007), 1001.

[8] I. Ass'ad , *J. of Applied Sciences*, **9**, (2009), 4056.

[9] M. Mermaz, F. Auger and B. Fernandez, *Phys. Rev. C* , **28**, (1983), 1587.

[10] A. Farra and I. Ass'ad, *J. Al-Azhar University –Gaza*, **7**, (2004), 63 .

[11] J. Werner, L. Leal, M. Munhoz, N. Carlin, L. Chamon, N. Added, J. Brage, R. Liguori, M. Coimbra, M. de Moura, F. Souza, A. Suaide, E. Szanto, A. de Toledo and J. akahashi, *Nucl. Phys. A* , **781**, (2007), 342.

[12] A. Farra, *Chinese J. OF Phys.* **46**, (2008), 416.

[13] M. Paul, S. Sanders, D. Geesaman, W. Henning, D. Kovar, C. Olmer and J. Schiffer, *Phys. Rev. C* , **21**, (1980), 1802.

[14] Z. Li, J. Su, B. Guo, Z.C. Li, X. Bai and J. Liu, Y. Li, S. Yan, B. Wang, Y. Wang, G. Lian, S. Zeng, E. Li, X. Fang, WLiu, Y. Chen, N. Shu and Q. Fan, *arXiv:0905.1530v1 [nucl-ex]* , (2009), 11 May.

[15] A. Belhout, S. Ouichaoui, H. Beaumevieille, A. Boughrara, S. Fortier, J. Kiener, J. Maison, S. Mehdi, L. Rosier, J. Thibaud, A. Trabelsi and J. Vernotte, *Nucl. Phys. A* , **793**, (2007), 178.

[16] A. Osman and A. Farra, *J. Phys. G. Nucl. Part. Phys.*, **15**, (1989), 871.

[17] A. Osman and A. Farra, *IL Nuovo Cimento A*, **103**, (1990), 1693.

[18] Y. Kondo and T. Tamura, *Phys. Rev. C*, **30**, (1984) 97.

[19] L. Xia and G. He, *Nucl. Phys. A*, **485**, (1988), 291.

[20] M . El-Azab and M. Hassanain, *Eur. Phys. J. A*, **19**, (2004), 231.

[21] A. Nadasen, M. McMaster, G. Gunderson, A. Judd, S. Villanueva, P. Schwandt, J. Winfieled, J. Van der Plicht, R. Warner, F. Becchetti and J. jänecke, *Phys. Rev. C*, **24**, (1988), 132.